

# Measuring similarity between trend behaviors of multivariate time series

WooCheol Jun,<sup>1</sup> Ayoung Park,<sup>2</sup> and Gabjin Oh<sup>2,\*</sup>

<sup>1</sup>*Hanwha Investment Trust Management, Seoul, 150-717, Korea*

<sup>2</sup>*Division of Business Administration,  
Chosun University Gwangju, 501-759, Korea*

(Dated: January 15, 2023)

## Abstract

We propose a novel approach for estimating the similarity between the trends of two time series, which has been an important problem in the fields of finance, economics and econophysics. We introduce the exit-time correlation (EC) to measure this similarity based on the exit-time method recently used as inverse statistics in financial time series analysis. We use a phase-noise induced Fourier transform method to illustrate the efficiency of our approach compared with the multiscale cross correlation method. The exit-time correlation serves as the inverse statistics for the multiscale cross correlation in analyzing correlation between multivariate time series. The application of our approach to high-frequency foreign exchange rates reveals that the exit-time correlation is related to time organization structure in interactions with a long-range time scale.

JEL : C39, G19

---

\*Electronic address: [phecogjoh@chosun.ac.kr](mailto:phecogjoh@chosun.ac.kr)

## I. INTRODUCTION

Recently, the study of time correlations in complex systems such as economic, financial and physical systems has provided us with a deeper insight into dynamical information and structures. These studies have used the correlation matrix to understand the overall structure in the dynamics of interactions between data in the system level, which is mainly constructed from the cross-correlation coefficients. However, the cross-correlation coefficient has a limitation in that it provides only information about interactions between two fluctuating time series in a short-range time scale. The subunits of complex systems in nature are often found to have interactions in a long-range time scale as well. Information about correlation between time series in a long-range time scale can provide deeper understanding of the dynamic interaction structure of complex systems.

In this paper, we introduce the exit-time correlation (EC) method that can measure a similarity between trend behaviors of multivariate time series. The trend behavior of the univariate time series has been studied through various statistical methods including the auto-correlation function, detrended fluctuation analysis (DFA) and multiscale trend analysis and is related to the correlation property in a long-range time scale. The relation between trend behaviors of multivariate time series has been investigated by using a moving average decomposition, a multivariate Fourier transform, wavelet analysis and cointegration, etc. However, these methods contain many control parameters and constraints, and so are not suitable for analyzing systems containing many multivariate subunits.

We extend the exit-time method to multivariate time series analysis in order to describe the degree of correlations between trend behaviors of time series. In the context of econophysics, the exit-time method was recently suggested, partly inspired by inverse statistics in turbulence, as an alternative for studying the distribution of waiting times needed to reach a fixed level of the return. The exit-time correlation method estimates correlations between exit-time series derived from multivariate time series, which produces correlation coefficient in the normalized region between  $-1$  and  $1$ .

We introduce a phase-noise induced Fourier transform method to generate time series with diverse correlations for a given trend behavior of the reference data, by adding noise to component signals in each frequency domain of the reference data. Using this method, we verify the usefulness of our exit-time correlation method in comparison with the multiscale cross

correlation (MCC). The exit-time correlation can be interpreted as the inverse statistics for multiscale cross correlation in analyzing correlations between multivariate time series. We apply our method to high-frequency foreign exchange (FX) rates and show that the correlation between trend behaviors of time series is related to the time organization structure in interactions between multivariate time series in a long-range time scale.

## II. EXIT-TIME CORRELATION METHOD

### A. Exit-time series

The exit-time method has been investigated as inverse statistics for financial time series and is defined as follows :

$$\tau_\rho = \inf\{\delta t = t_2 - t_1 : \delta s = s(t_2) - s(t_1) \geq \rho, t_2 > t_1\}, \quad (1)$$

where the  $s(t)$  is a log price at time  $t$ . The inverse statistics investigates the effects of intermittency in fully developed turbulence by averaging moments of the distance as a function of a fixed velocity difference. This method proposes an alternative way for describing and analyzing a turbulent velocity field by inverting the structure function equation. The exit-time method considers the distribution of minimal time  $\tau_\rho$  to reach a fixed level of return  $\rho$  instead of studying the distribution of returns  $\delta s$  as a function of a fixed time period  $\delta t$ .

The previous works uncovered a novel stylized fact in financial time series that the distribution of exit-time  $\tau_\rho$  follows a power law,  $p(\tau_\rho) \sim \tau_\rho^{-\alpha}$ , with  $\alpha \approx 1.5$  for large  $\tau_\rho$  universally. Moreover, for fractional Brownian motion with a Hurst exponent  $H$  the distribution of exit-times exhibits scaling behavior of  $p(\tau_\rho) \sim \tau_\rho^{-(2-H)}$  for large  $\tau_\rho$ . The financial time series has been usually regarded as a random walk with the Hurst exponent  $H$  ( $\sim 0.5$ ). Therefore, the statistics of the distribution  $p(\tau_\rho)$  can give information on the trend behavior of a given time series.

In our method, the exit-time series  $\tau_\rho(t)$  is derived from the exit-time method in Eq. (1)

as follows :

$$\begin{aligned}
\tau_{\rho}^{+} &= \inf\{\tau^{+} : \delta s = s(t + \tau^{+}) - s(t) \geq \rho\} \\
\tau_{\rho}^{-} &= \inf\{\tau^{-} : \delta s = s(t + \tau^{-}) - s(t) \leq -\rho\}, \\
\tau_{\rho}(t) &= \begin{cases} \tau_{\rho}^{+}, & \text{if } \tau_{\rho}^{+} < \tau_{\rho}^{-} \\ -\tau_{\rho}^{-}, & \text{if } \tau_{\rho}^{+} > \tau_{\rho}^{-} \\ 0, & \text{if } \tau_{\rho}^{+}, \tau_{\rho}^{-} \rightarrow \infty \quad (\rho > 0, t = 1, 2, \dots, N), \end{cases} \quad (2)
\end{aligned}$$

where  $s(t)$  is a time series with a trend behavior (Fig. 1) and  $\tau_{\rho}^{+}(\tau_{\rho}^{-})$  is a minimal time span needed for the difference  $\delta s$  to exceed  $\rho(-\rho)$ . The exit-time series  $\tau_{\rho}(t)$  gives information on whether the first event of the signal  $s(t)$  is  $s(t) + \rho$  or  $s(t) - \rho$  after time  $t$ . In Fig. 1, the signal  $s(t)$  reaches  $s(t_1) + \rho(s(t_2) - \rho)$  for the first time after time  $t_1(t_2)$ , and hence the value of exit-time  $\tau_{\rho}(t)$  is  $\tau_1(-\tau_2)$  at time  $t_1(t_2)$ .

The exit time series  $\tau_{\rho}(t)$  becomes 1 or  $-1$  in ascending or descending trends of  $s(t)$ , respectively, for very small  $\rho$ . As  $\rho$  increases,  $\tau_{\rho}(t)$  describes the trend behavior of  $s(t)$  in a long-range time scale. The domination of small  $|\tau_{\rho}(t)|$  implies a steeply ascending or descending trend, while large  $|\tau_{\rho}(t)|$  indicates a long-lasting trend. Since there can be no event to reach  $s(t) + \rho$  or  $s(t) - \rho$  as  $t$  approaches  $N$ , we define the exit time  $\tau_{\rho}(t)$  as zero in this case.

## B. Exit-time Correlation

In this section, we introduce the exit-time correlation method, which estimates the degree to which the whole trends of two time series are correlated.

When the exit time series  $\tau_{\rho}(t)$  is positive(negative), the absolute value  $|\tau_{\rho}(t)|$  is inversely proportional to the slope of the ascending(descending) trend of time series  $s(t)$  for a given fluctuation range  $\rho$ . We rescale the original signals,  $s_1(t)$  and  $s_2(t)$ , to normalize the range of  $\rho$  into the unit interval before deriving exit-time series,  $\tau_{\rho}^1(t)$  and  $\tau_{\rho}^2(t)$ , as follows :

$$\begin{aligned}
s_1'(t) &= \frac{s_1(t) - \min(s_1)}{\max(s_1) - \min(s_1)} \\
s_2'(t) &= \frac{s_2(t) - \min(s_2)}{\max(s_2) - \min(s_2)} \quad (t = 1, 2, \dots, N), \quad (3)
\end{aligned}$$

where the functions,  $\min(s(t))$  and  $\max(s(t))$ , give the minimum and maximum values of time series  $s(t)$  for all time  $t$ , respectively. Therefore, the rescaled signals,  $s'_1(t)$  and  $s'_2(t)$ , and  $\rho$  can be normalized into the unit interval of  $[0, 1]$  as shown in Fig. 1. The exit-time correlation  $C_E(\rho)$  estimates the similarity between exit time series  $\tau_\rho^1(t)$  and  $\tau_\rho^2(t)$  derived from  $s'_1(t)$  and  $s'_2(t)$ , for a given scale  $\rho$ . First, we define the strength of similarity  $X(t)$  between  $\tau_\rho^1(t)$  and  $\tau_\rho^2(t)$  at time  $t$  for a given scale  $\rho$  as follows :

$$X(t) = \begin{cases} \frac{\min\{\tau_\rho^1(t), \tau_\rho^2(t)\}}{\max\{\tau_\rho^1(t), \tau_\rho^2(t)\}} & \text{if } \tau_\rho^1(t)\tau_\rho^2(t) \neq 0 \\ 0 & \text{otherwise.} \end{cases}$$

Then  $X(t)$  exists on the interval of  $[-1, 1]$  and the exit-time correlation  $C_E(\rho)$  for a given scale  $\rho$  is defined by

$$C_E(\rho) = \frac{1}{N-T} \sum_{t=1}^N X(t) \quad (0 < \rho < 1),$$

$$T = \sum_{t=1}^N (1 - |\text{sign}(\tau_\rho^1(t)\tau_\rho^2(t))|), \quad (4)$$

where the value of function  $\text{sign}(x)$  becomes  $-1$ ,  $0$  and  $1$  when  $x < 0$ ,  $x = 0$  and  $x > 0$ , respectively. Therefore, the  $C_E(\rho)$  is the average of  $X(t)$  during the time periods with non-zero  $\tau_\rho^1(t)\tau_\rho^2(t)$ . As  $X(t)$  approaches  $1(-1)$ , the two time series,  $s_1(t)$  and  $s_2(t)$ , tend to have a similar time span to reach the same(opposite) fluctuation range  $\rho$  after time  $t$ . Consequently, the  $C_E(\rho)$  also lies between  $-1$  and  $1$ , and estimates the similarity between slopes of ascending or descending trends of  $s_1(t)$  and  $s_2(t)$  within a fluctuation range  $\rho$ . Note that  $C_E(\rho)$  approaches  $1(-1)$  and  $0$  when the trend behaviors of  $s_1(t)$  and  $s_2(t)$  are correlated(anti-correlated) and uncorrelated, respectively.

### III. ESTIMATING SIMILARITY BETWEEN TREND BEHAVIORS OF MULTIVARIATE TIME SERIES

#### A. Phase-noise induced Fourier transform

We introduce a phase-noise induced Fourier transform method to generate time series with diverse correlation properties for the trend behavior of the reference signal. This method

considers correlation in a frequency domain, inspired by the Fourier surrogate method for discrete time series sampled at evenly spaced time intervals as follows :

$$\begin{aligned}
s(t) &= \sum_{k=0}^{N-1} c_k \exp[i(\frac{2\pi k}{N}t + \phi_k)], \\
\bar{s}(t) &= \sum_{k=0}^{N-1} c_k \exp[i(\frac{2\pi k}{N}t + \phi_k)] \exp(i\alpha_k) \\
& \quad ( t = 0, 1, 2, \dots, N-1, \quad N = 2^\eta ),
\end{aligned} \tag{5}$$

where the phase  $\phi_k$  of the signal  $s(t)$  has a symmetry of  $\phi_k = -\phi_{N-k}$  for  $2^{(\eta-1)} < k \leq 2^\eta - 1$ , and  $\alpha_k$  are independent random numbers with a uniform distribution in  $[0, 2\pi]$  and the same symmetry as  $\phi_k$ . After the randomization of the Fourier phases  $\phi_k$  of  $s(t)$ , this method generates a signal  $\bar{s}(t)$  with the same linear features as  $s(t)$  but without nonlinearities, while preserving the amplitude  $c_k$  of the Fourier transform.

We can generate a signal  $\bar{s}(t)$  with diverse correlations for trend behavior of the reference signal  $s(t)$  by controlling the magnitudes of random phases  $\alpha_k$  in each frequency domain as follows :

$$\alpha_k = \begin{cases} 0 & \text{if } 0 < k \leq 2^{(\eta-1)-k'} \\ iid(0, 2\pi) & \text{if } 2^{(\eta-1)-k'} < k \leq 2^{(\eta-1)} - 1 \quad ( 0 < k' < \eta - 1 ), \end{cases} \tag{6}$$

where  $iid(0, 2\pi)$  denotes independent identically distributed random numbers between 0 and  $2\pi$ . In Eqs. (5) and (6), the phases  $\phi_k$  of signal components of the original signal  $s(t)$  in a high frequency domain with  $2^{(\eta-1)-k'} < k \leq 2^{(\eta-1)} - 1$  are randomized by  $\alpha_k$ , whereas the phases in the low frequency domain with  $0 < k \leq 2^{(\eta-1)-k'}$  are conserved.

Therefore, the signal components of  $\bar{s}(t)$  have the same trend behaviors as ones for  $s(t)$  in the low frequency domain. As the randomization level  $k'$  increases, the signal  $\bar{s}(t)$  behaves more heterogeneously with respect to the reference signal  $s(t)$ , beginning from the high frequency components and moving to the lower ones.

Fig. 2 shows that the similarity between trend behaviors of  $s(t)$ (solid line) and  $\bar{s}(t)$ (dotted line) is destroyed as  $k'$  increases. We generated a random walk signal as the reference signal  $s(t)$  with a Hurst exponent  $H$  ( $= 0.5$ ) and a signal length  $\eta = 17$  in Eq. (5) by using the relation  $|c_k|^2 \sim k^{-2H-1}$ .

## B. Multiscale cross correlation

We compare the multiscale cross correlation and exit-time correlation method for classifying the similarity between trend behaviors of  $s(t)$  and  $\bar{s}(t)$  depending on  $k'$ . The multiscale cross correlation measures the correlation between fluctuations of two time series on a fixed time scale  $\tau$  as follows :

$$C_M(\tau) = \frac{\langle (\Delta s_1 - \langle \Delta s_1 \rangle)(\Delta s_2 - \langle \Delta s_2 \rangle) \rangle}{\sigma_1(\tau)\sigma_2(\tau)}, \quad (7)$$

where the signals  $\Delta s_1$  and  $\Delta s_2$  are defined as

$$\begin{aligned} \Delta s_1(t, \tau) &= s_1(t + \tau) - s_1(t) \\ \Delta s_2(t, \tau) &= s_2(t + \tau) - s_2(t) \quad (t = 1, 2, \dots, N - \tau). \end{aligned} \quad (8)$$

In Eq. (7), the quantities  $\sigma_1(\tau)$  and  $\sigma_2(\tau)$  correspond to the standard deviations of  $\Delta s_1(t, \tau)$  and  $\Delta s_2(t, \tau)$ , respectively. The multiscale cross correlation  $C_M(\tau)$  lies in  $[-1, 1]$  and approaches  $1(-1)$  as  $s_1(t)$  and  $s_2(t)$  become correlated(anticorrelated) for fluctuations on time scale  $\tau$ . The exit-time correlation  $C_E(\rho)$  estimates the correlation between two time series on a fixed fluctuation scale  $\rho$ , so that it can be interpreted as inverse statistics for  $C_M(\tau)$  in analyzing the correlation between two time series.

The  $s(t)$  and  $\bar{s}(t)$  are generated as random walk signals with length  $N = 2^{17}(\eta = 17)$  by Eqs. (5) and (6). The twenty samples of  $\bar{s}(t)$  for a reference signal  $s(t)$  are generated for each randomization level  $k'$ . The  $C_E(\rho)$  and  $C_M(\tau)$  are estimated on varying scales  $\rho$  and  $\tau$ , respectively, for  $s(t)$  and  $\bar{s}(t)$ . Fig. 3 shows  $C_M(\tau)$  for  $\tau = 1$  between  $s(t)$  and twenty sample  $\bar{s}(t)$  signals as the randomization level  $k'$  is varied from 8 to 15 with an increment of 0.5 in Eq. (6). The plotted symbols and errorbars represent mean values and standard deviations derived from twenty values of  $C_M(1)$  for each  $k'$ . The  $C_M(1)$  is the same as the cross-correlation coefficient (Eq. (7)) and cannot classify the variations in similarity between trend behaviors of  $s(t)$  and  $\bar{s}(t)$  for large  $k'$  well.

Fig. 4 shows  $C_E(\rho)$  and  $C_M(\tau)$  for varying scales of  $\rho$  and  $\tau$  as  $k'$  is increased. The plotted symbols and errorbars correspond to mean values and standard deviations of twenty samples of  $C_E(\rho)$  and  $C_M(\tau)$  as in Fig. 3. In Fig. 4(a), the  $C_E(\rho)$  for small  $\rho$  ( $= 0.02$ ) converges close to zero as for  $C_M(1)$  in Fig. 3 because  $C_E(\rho)$  reflects the correlation between fluctuations of  $s(t)$  and  $\bar{s}(t)$  in a short time scale for small  $\rho$ .

However,  $C_E(\rho)$  decreases monotonically as the scale  $\rho$  increases, so that it classifies the variations in similarity between trend behaviors of  $s(t)$  and  $\bar{s}(t)$  as a function of  $k'$  well as in Fig. 2. On the other hand,  $C_M(\tau)$  exhibits similar behaviors for all scales  $\tau$ , nearly saturating for  $k' \geq 11$  and cannot detect the effect of  $k'$  on the correlation between  $s(t)$  and  $\bar{s}(t)$  sufficiently. Note that the  $s(t)$  and  $\bar{s}(t)$  for  $k' = 11$  in Fig. 2 exhibit similar large scale trend behavior. Fig. 5 shows that  $C_E(\rho)$  reflects the variation of correlations between  $s(t)$  and  $\bar{s}(t)$  more effectively than  $C_M(\tau)$  for large  $k'$ . The increase in standard deviations of  $C_E(\rho)$  and  $C_M(\tau)$  as a function of  $k'$  in Fig. 5 may be caused by an instability in the signal  $\bar{s}(t)$  due to the noise level growth.

In Eq. (4),  $C_E(\rho)$  is not dependent on the size of fluctuations of  $s_1(t)$  and  $s_2(t)$  since it restricts the range of fluctuations within an interval,  $[-\rho, \rho]$ , whereas  $C_M(\tau)$  in Eq. (7) reflects the information about magnitudes of fluctuations of  $s_1(t)$  and  $s_2(t)$  for scale  $\tau$ . The different results in  $C_E(\rho)$  and  $C_M(\tau)$  in Figs. 4 and 5 may originate from this difference.

### C. The exit-time correlation for foreign exchange rates

This section applies the exit-time correlation method to multivariate foreign exchange (FX) rates and investigate the relation between correlation structures, detected by  $C_E(\rho)$ , with linear correlations ( $C_M(1)$ ) between these data.

In Fig. 6(a), four foreign exchange rate signals with very similar trend behaviors are shown. The dashed line in Fig. 6(b) corresponds to  $C_E(\rho)$  with  $\rho=0.2$  for all pairs of foreign exchange rate data. We applied a multivariate random-shuffle surrogate method to investigate the time-organization structure of correlation detected by  $C_E(\rho)$ . The random shuffle surrogate method has been proposed to investigate whether a univariate fluctuation signal has some kind of dynamic structure. This method is extended to multivariate time series analysis as follows.

In Eq. (8), the fluctuations,  $\Delta s_1(t, 1)$  and  $\Delta s_2(t, 1)$ , are randomized by the same random time index  $g(t)$ , producing surrogate fluctuation signals,  $\Delta s_1(g(t), 1)$  and  $\Delta s_2(g(t), 1)$ . The random integer sequence  $g(t)$  has a one-to-one correspondence with all integers between 1 and  $N - 1$ . Then, the cross correlation ( $C_M(1)$ ) between surrogate fluctuation signals is the same as the cross correlation between original fluctuation signals and the distribution of each fluctuation signal is conserved. We reconstruct surrogate signals  $s'_1(t)$  and  $s'_2(t)$  by integrat-



ing  $\Delta s_1(g(t), 1)$  and  $\Delta s_2(g(t), 1)$  cumulatively. We generate twenty surrogate pairs for each possible pair of signals and test the null hypothesis that the statistics estimated by  $C_E(\rho)$  can be fully described by a linear correlation structure ( $C_M(1)$ ) between two signals. The symbols plotted on the dotted line in Fig. 6(b) represent the mean values of  $C_E(\rho)$  derived from twenty surrogate pairs with the errorbar corresponding to the 95 percent confidence region for the null hypothesis. Fig. 6(b) suggests that the null hypothesis is rejected for all cases and the correlation estimated from  $C_E(\rho)$  is related to a time organization structure which cannot be detected by a linear cross correlation method.

#### IV. CONCLUSION

In summary, we introduced an exit-time correlation method which estimates the degree of similarity between trend behaviors of multivariate time series. This method measures the correlation between the exit time series derived from original multivariate time series in a normalized region between  $-1$  and  $1$ . We have shown that the exit time correlation  $C_E(\rho)$  efficiently reflects the variations in correlation between test time series which cannot be detected well by a linear cross correlation as in the cases of foreign exchange rates.

The cross correlation matrix has been used to investigate a dynamical correlation structure in the interactions between data in the system level. However, the cross correlation provides only information about correlations in a short range time scale. The exit time correlation estimates correlations between multivariate time series in a long range time scale and can be quantified in a normalized region between  $-1$  and  $1$  like as the cross correlation coefficient. Therefore, the exit time correlation matrix can be constructed and provide the information about dynamical correlation structure in interactions between subunits of complex systems in a long range time scale. In particular, the studies of the topological structure in the cross correlation matrix between financial time series have been exploited. We can obtain more information about the macroscopic market structure from analysis of dynamic interactions between financial time series based on the exit time correlation matrix. Moreover, we expect that this information can be applied to portfolio optimization and optimal hedging analysis in econometrics.

## V. ACKNOWLEDGEMENTS

---

- [1] V. Plerou *et al.*, Phys. Rev. E **65**, 066126 (2002); P. Šeba, Phys. Rev. Lett. **91**, 198104 (2003); J.-P. Onnela, K. Kaski and J. Kertész, Eur. Phys. J. B **38**, 353 (2004); M. S. Santhanam and Holger Kantz, Phys. Rev. E **69**, 056102 (2004); F. Luo, J. Zhong, Y. Yang and J. Zhou, Phys. Rev. E **73**, 031924 (2006).
- [2] M. Bartolozzi and A. W. Thomas, Phys. Rev. E **69**, 046112 (2004); M. Argollo de Menezes and A.-L. Barabási, Phys. Rev. Lett. **93**, 068701 (2004); Y. Yokoya, Phys. Rev. E **69**, 016121 (2004).
- [3] I. Zaliapin, A. Gabrielov and V. Keilis-Borok, arXiv:physics/0305013 (2003); I. Zaliapin *et al.*, Pure appl. geophys. **162**, 827 (2005).
- [4] R. F. Engle and C. W. J. Granger, Econometrica **55**, 251 (1987); T. Ula, J. Time Series Anal. **14**, 645 (1993); M. Paluš, Phys. Lett. A **213**, 107 (1996); F. Aparisi and J. C. Garcia-Diaz, Comput. Oper. Res. **31**, 1437 (2004); A. R. Soltan and A. Parvardeh, Stoch. Proc. Appl. **115**, 1838 (2005).
- [5] R. N. Mantegna and H. E. Stanley, *An introduction to Econophysics : Correlation and Complexity in finance* (Cambridge Univ. Press, Cambridge, 1999).
- [6] M. H. Jensen, Phys. Rev. Lett. **83**, 76 (1999); L. Biferale *et al.*, Phys. Rev. Lett. **87**, 124501 (2001).
- [7] M. H. Jensen, A. Johansen and I. Simonsen, Physica A **324**, 338 (2003); M. H. Jensen, A. Johansen and I. Simonsen, J. Mod. Phys. B **17**, 4003 (2003); M. Montero *et al.*, Phys. Rev. E **72**, 056101 (2005); W.-X. Zhou and W.-K. Yuan, Physica A **353**, 433 (2005).
- [8] E. Laciari, IEEE T. Bio.-Med. Eng. **50**, 344 (2003).
- [9] The foreign exchange (FX) rate data are from the Olsen and Associates with four global spot FX rates (Fig. 6(a)). The data run from 1. January 1996 GMT to 31. December 1996 GMT with 12524 records at half hour intervals.
- [10] M.-Z. Ding and W.-M. Yang, Phys. Rev. E **52**, 207 (1995).
- [11] J.-P. Bouchaud and M. Potters, *Theory of Financial Risk : From Statistical Physics to Risk Management* (Cambridge University Press, Cambridge, 2000); J. Voit, *The Statistical Me-*

- chanics of Financial Markets* (Springer, New York, 2001).
- [12] T. Schreiber and A. Schmitz, *Physica D* **142**, 346 (2000).
- [13] J. Feder, *FRACTALS* (Plenum Press, New York, 1988).
- [14] G. Bonanno, N. Vandewalle and R. N. Mantegna, *Phys. Rev. E* **62**, 7615 (2000); G. Bonanno, G. Caldarelli, F. Lillo and R. N. Mantegna, *Phys. Rev. E* **68**, 046130 (2003); F. Lillo and R. N. Mantegna, *Phys. Rev. E* **72**, 016219 (2005).
- [15] C. Alexander, *Phil. Trans. R. Soc. Lond. A* **357**, 2039 (1999); S. Pafka and I. Kondor, *Physica A* **343**, 623 (2004); C. L. Dunis and R. Ho, *J. Asset Manage.* **6**, 33 (2005); F. Fabozzi, S. M. Focardi and P. N. Kolm, *Financial modeling of the Equity market : From CAPM to Cointegration* ( John Wiley Sons, New Jersey, 2006).

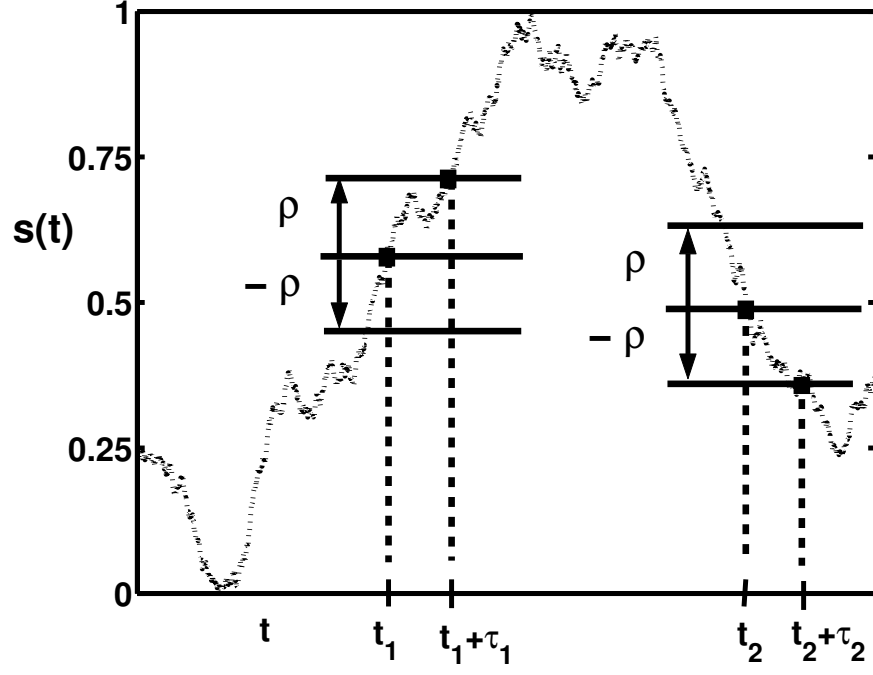


FIG. 1: The exit time  $\tau_\rho(t)$  at  $t_1$  and  $t_2$  for a signal  $s(t)$  :  $\tau_\rho(t_1) = \tau_1$ ,  $\tau_\rho(t_2) = -\tau_2$ .  $s(t)$  is a rescaled signal from its original signal by Eq. (3).

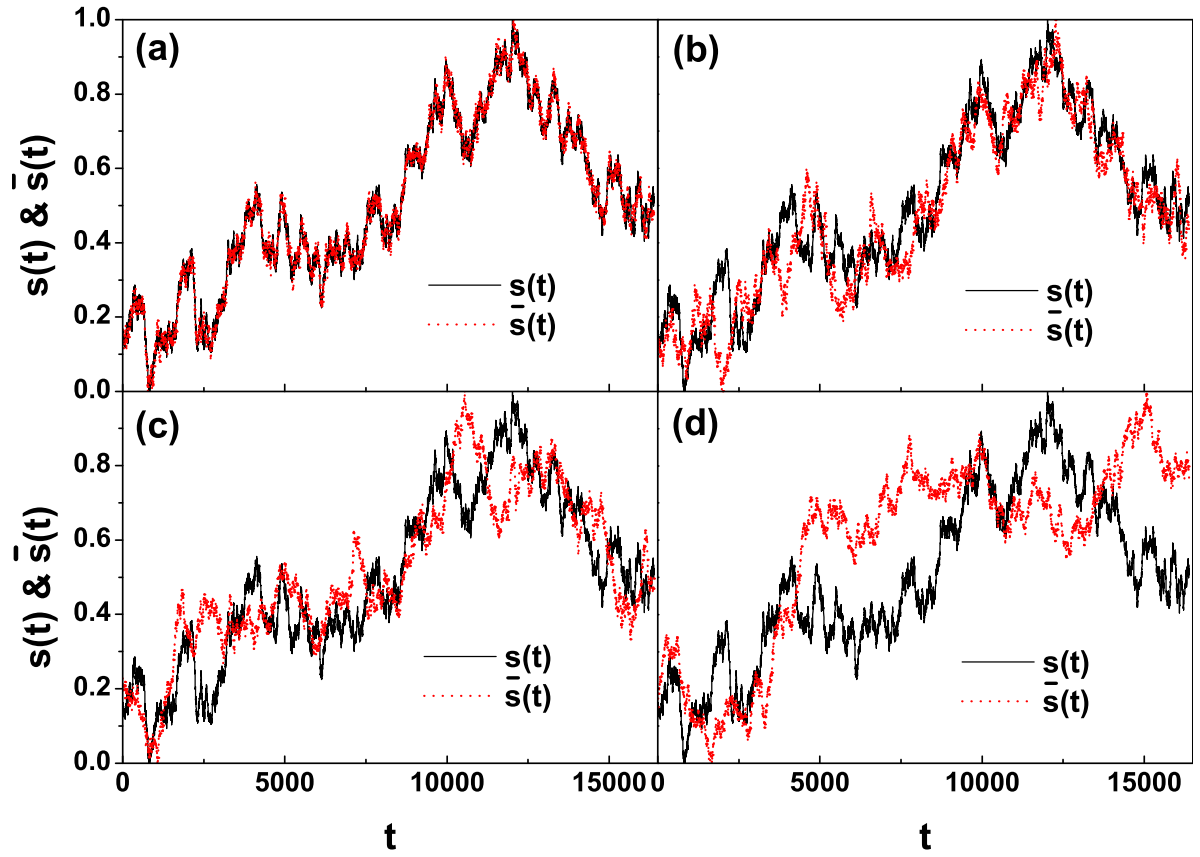


FIG. 2: Typical examples of  $s(t)$  (black solid) and  $\bar{s}(t)$  (red dotted) for different randomizing levels ( $k'$ ). The lengths ( $N$ ) of  $s(t)$  and  $\bar{s}(t)$  are  $2^{17}$  ( $\eta = 17$ ) in Eq. (5). We represented first  $2^{14}$  data points in this figure : (a)  $k' = 8.0$  (b)  $k' = 11.0$  (c)  $k' = 12.0$  (d)  $k' = 14.0$ .

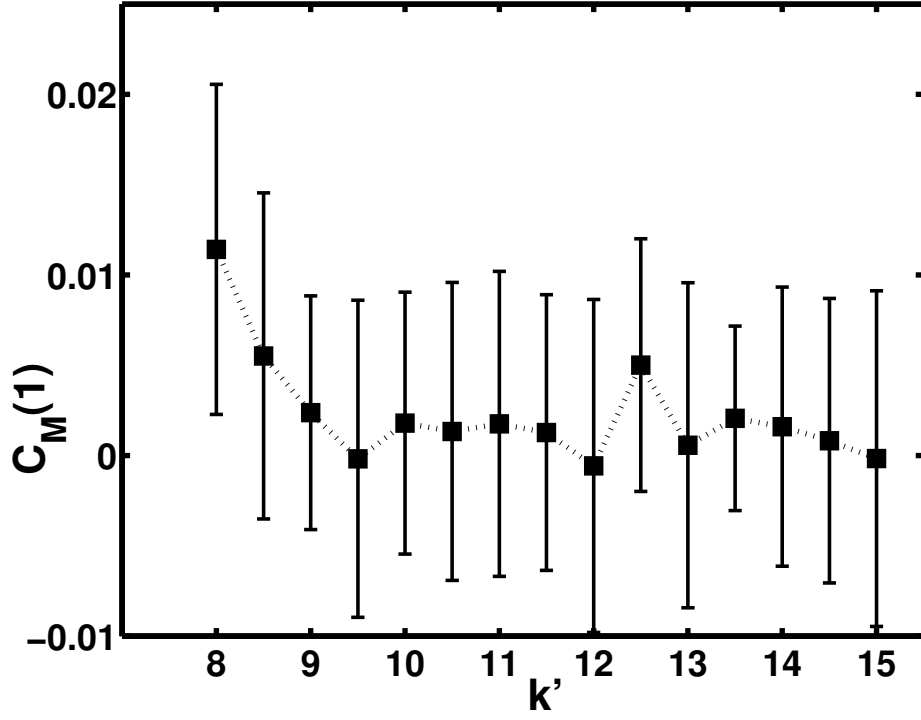


FIG. 3: The cross correlation coefficients with  $\tau = 1$  between  $s(t)$  and twenty  $\bar{s}(t)$ , averaged over twenty samples, in Eqs. (5) and (6). The symbols(■) and errorbars correspond to the mean values and the standard deviations derived from all pairs for each  $k'$ .

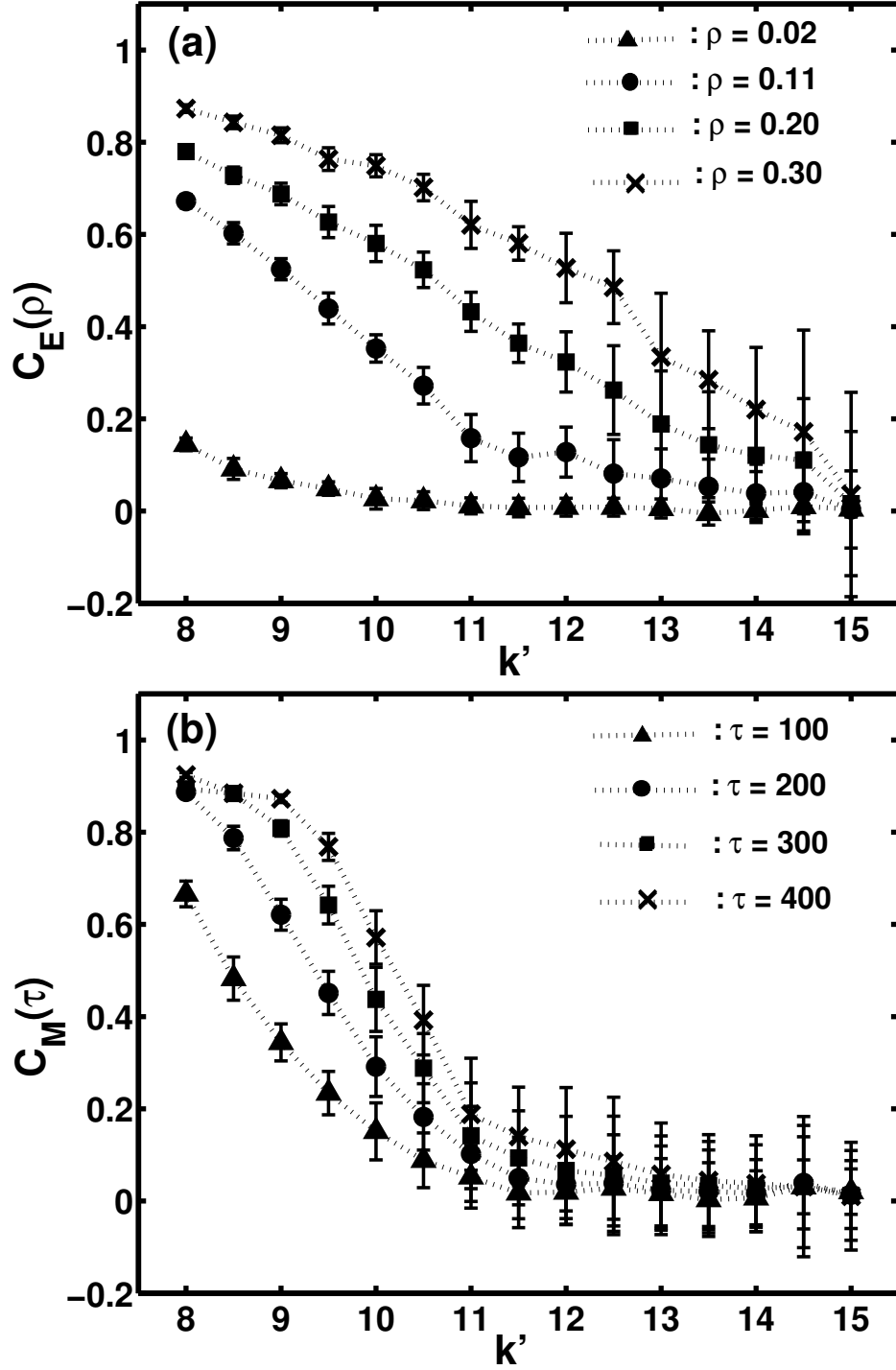


FIG. 4: (a)  $C_E(\rho)$  as a function of the randomization level  $k'$  for scales  $\rho(= 0.02, 0.11, 0.2$  and  $0.3)$ . (b) The variation of  $C_M(\tau)$  for  $k'$  with scales  $\tau(= 100, 200, 300$  and  $400)$ . The plotted symbols and errorbars correspond to mean values and standard deviations derived from all pairs in each  $k'$ .

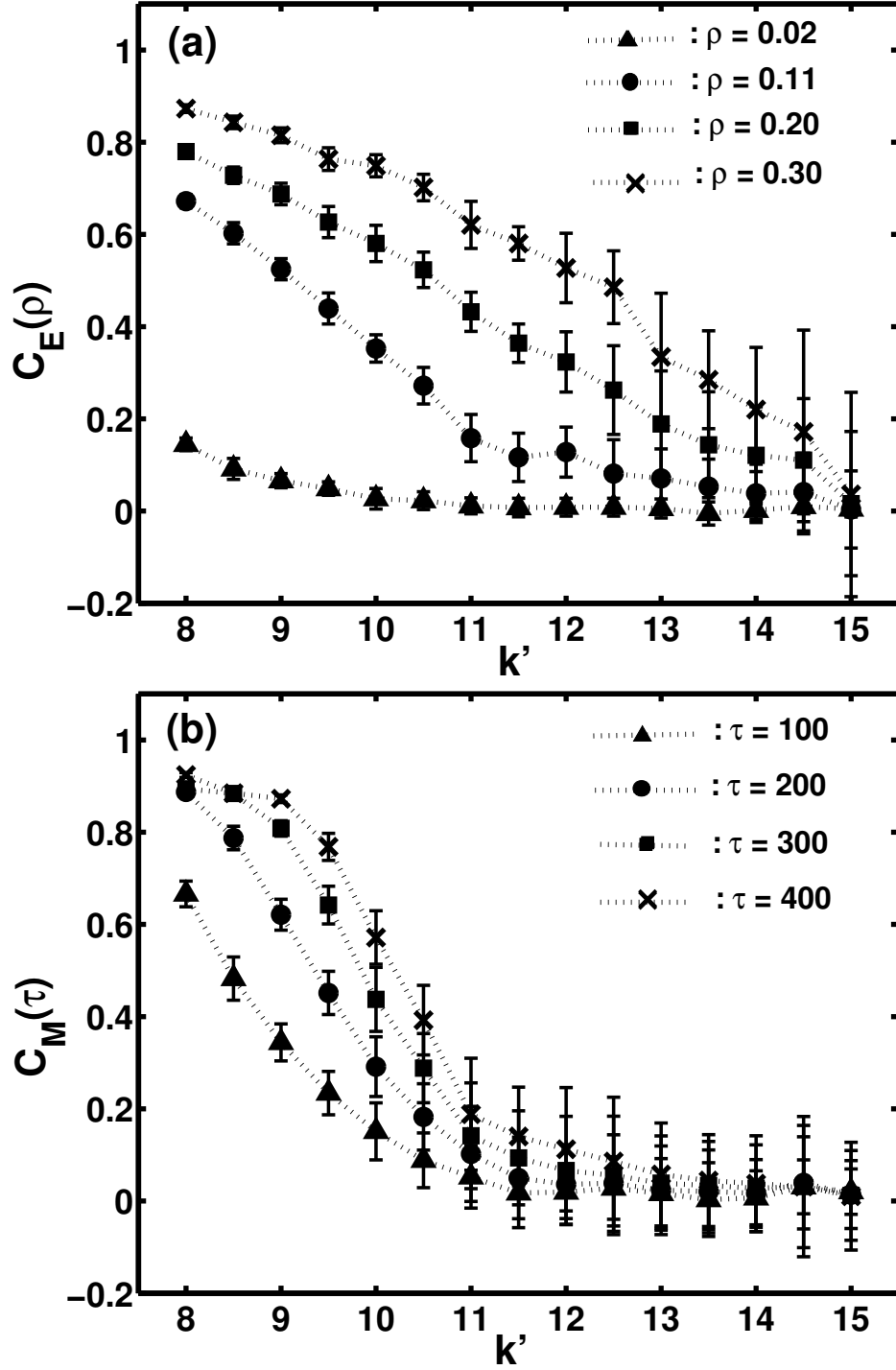


FIG. 5: (a)  $C_E(\rho)$  as a function of the randomization level  $k'$  for scales  $\rho$  ( $= 0.02, 0.11, 0.2$  and  $0.3$ ). (b) The variation of  $C_M(\tau)$  for  $k'$  with scales  $\tau$  ( $= 100, 200, 300$  and  $400$ ). The plotted symbols and errorbars correspond to mean values and standard deviations derived from all pairs in each  $k'$ .



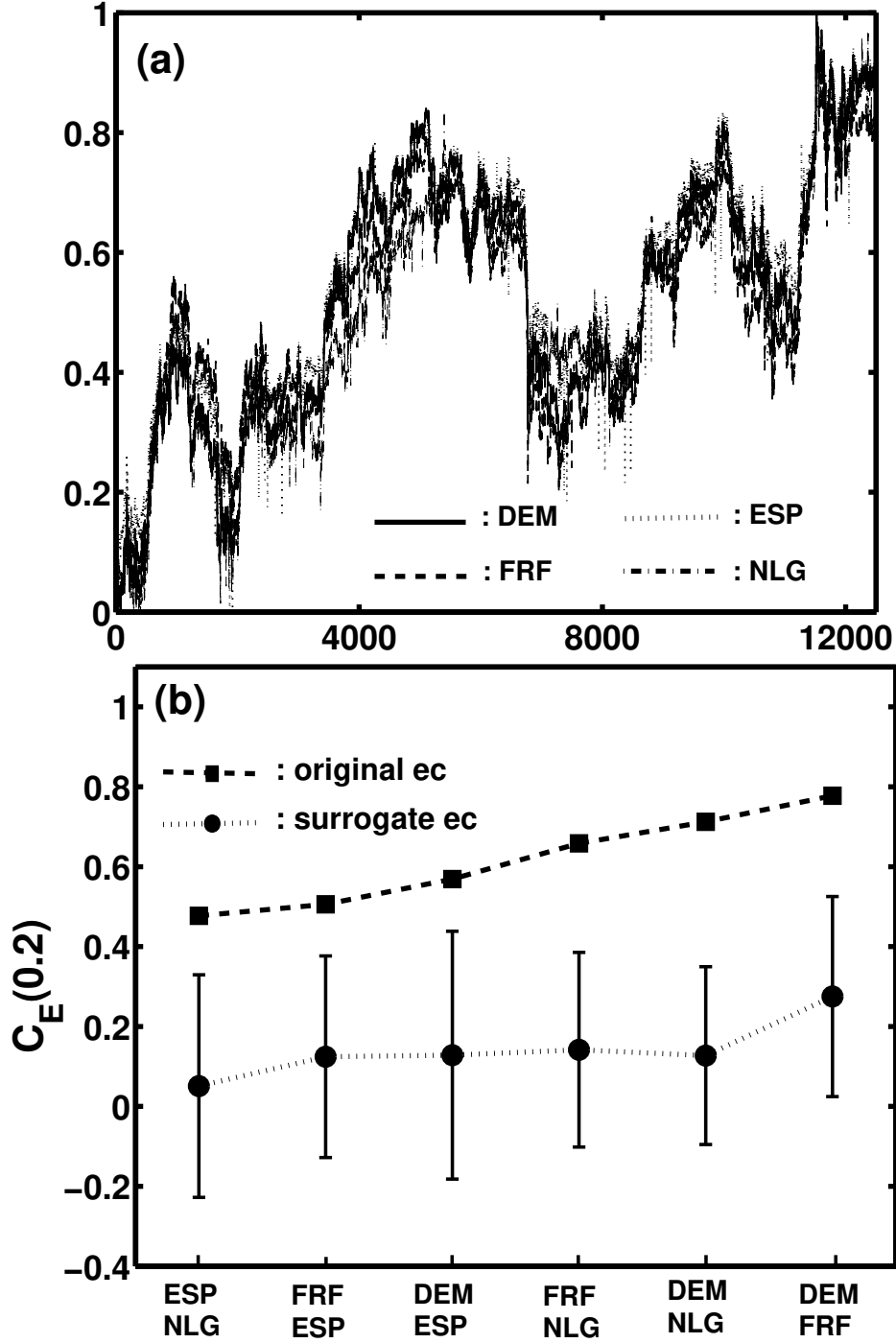


FIG. 6: (a) The representation of foreign exchange (FX) rates for the U.S. dollar : DEM(Germany), ESP(Spain), FRF(France) and NLG(Netherlands) [9]. The signals are rescaled by Eq. (3) from the originals. (b) The exit time correlation for pairs between original signals (■) and between multivariate shuffled signals (●). The plotted symbols (●) and errorbars correspond to mean values and the 95 percent confidence region for the null hypothesis derived from twenty surrogate pairs.